Methodology Development for Investigation of Slurry Abrasion Corrosion by Integrating an Electrochemical Cell to a Miller Tester

Sheng-Hui Wang[1]*, Jiaren Jiang[1]*, and Margaret M. Stack[2]

[1] Mining Wear and Corrosion
Energy, Mining and Environment Portfolio
National Research Council Canada
4250 Wesbrook Mall, Vancouver, BC V6T 1W5, Canada

[2] Department of Mechanical Engineering
University of Strathclyde
75 Montrose St., Glasgow, G1 1XJ, United Kingdom

* Corresponding authors:
Email: sheng-hui.wang@nrc-cnrc.gc.ca
jiaren.jiang@nrc-cnrc.gc.ca
Fax: (+1) 604-221-3001

Abstract

Material losses in slurry handling systems constitute a significant fraction of cost in oil sands, mining, and mineral processing operations. It is thus important to better understand wear attack mechanisms and major factors affecting wear in such applications. In this work, a methodology and a testing system have been developed to study the abrasion-corrosion synergism during slurry abrasion based on a Miller test machine by incorporating a three-electrode electrochemical cell. The proposed methodology has then been validated experimentally using QT 100 steel. It has been shown that cathodic protection by using such system setup is effective in suppressing the corrosion effect on the total material loss. In general, corrosion-induced enhancement on slurry abrasion loss rate increases with slurry corrosivity but inversely with sliding speed. Slurry corrosivity appears to play a more important role.

Keywords:

Slurry abrasion; abrasion-corrosion; tribo-corrosion; Miller tester

1. Introduction

Slurry abrasion is commonly encountered in slurry handling equipment used in the oil sands, mining and mineral processing operations, such as slurry pumps, separation vessels and systems and hydrotransport pipelines. The related cost on equipment maintenance and production interrupt can be very significant. There are thus strong demands from the industry to better understand the underlining slurry abrasion mechanisms and to find practical solutions for mitigating the related severe damages.

Wear mechanisms in slurry handling systems are fairly complex and are not fully understood. Nevertheless, corrosion is almost always involved in the slurry abrasion of such systems because the water used in most of the processes typically contains various types of corrosive species, such as chlorides and other species from the minerals being processed as well as from the processing agents [1-4]. Many researches have shown that synergistic effect can significantly increase the total materials loss under combined wear and corrosion attacks in different wear or erosion systems [1, 2, 5-13]. In the past two decades or so, extensive researches have been dedicated to the so-called tribo-corrosion phenomena and remarkable progresses have been made in understanding the synergistic effect [14-25]. However, so far there is still a lack of effective evaluation tools for the study of abrasion-corrosion in slurry abrasion and little has been done to address the practically important issue [26].

Among few available laboratory testing methods for slurry abrasion studies, Miller tester is an established tool for evaluating the slurry abrasivity as well as for ranking the wear performance of materials in given slurry conditions [27]. In this work, a Miller tester has been modified to establish a methodology for investigating the slurry abrasion-corrosion synergism. A preliminary investigation has been performed on a QT 100 steel rate to validate the methodology and to have a preliminary investigation of the significance of corrosion-induced enhancement to wear.

2. Methodology Development

2.1 The Miller tester and the testing methodology

The testing methodology is developed based on a Miller tester, which was constructed in conformity to the ASTM G75 standard as shown in Fig. 1a. The tester has four parallel identical testing cells. Each cell consists of a slurry bath and a reciprocating arm with a stroke of 203 mm, as schematically shown in Fig, 1b. A wear specimen having a testing surface area of 12.7mm x 25.4 mm is installed on a specimen holder attached to the arm and is loaded against a neoprene rubber lap at the bottom of the slurry bath. More detailed description of the test machine can be referred to the ASTM G75 standard [27]. It should be noted that the neoprene rubber lap is much more wear resistant under the abrasion condition employed and that there should be no measureable effect on testing results as far as the neoprene rubber lap is well maintained.

(a)

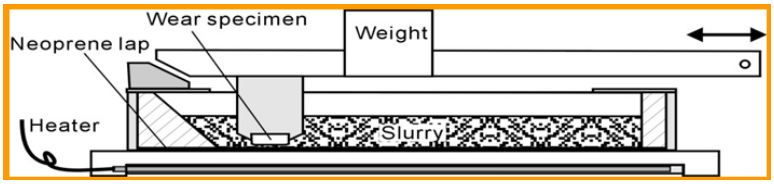

(b)

Fig. 1 The Miller testing machine (a), and schematic diagram showing the working principle (b)

In order to acquire the individual contributions of abrasion, corrosion and synergy, an in-situ three-electrode electrochemical corrosion cell is implemented in the Miller tester as shown in Fig. 2a. The working electrode (i.e., the specimen) immersed in the testing slurry and the counter electrode are connected to a potentiostat. A reference electrode (in this case, a saturated calomel electrode) is placed in a holder that is fixed on the pivoted reciprocating arm and travels together with the wear specimen.

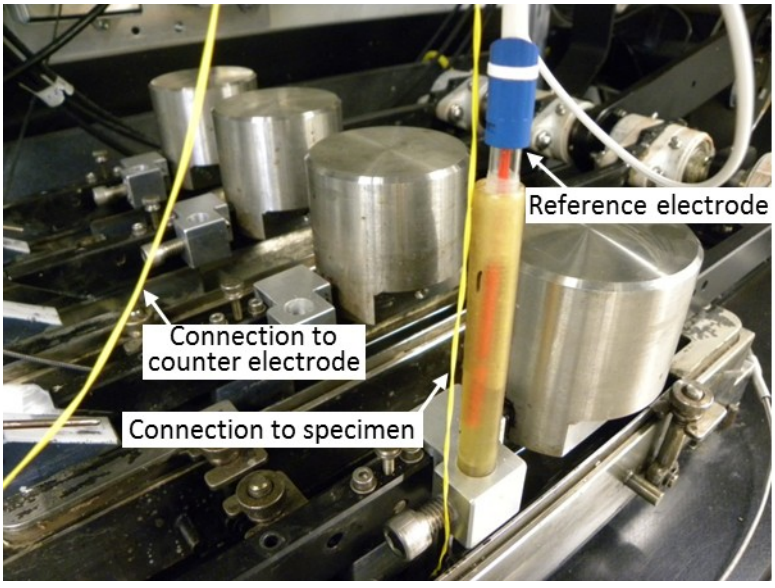

(a)

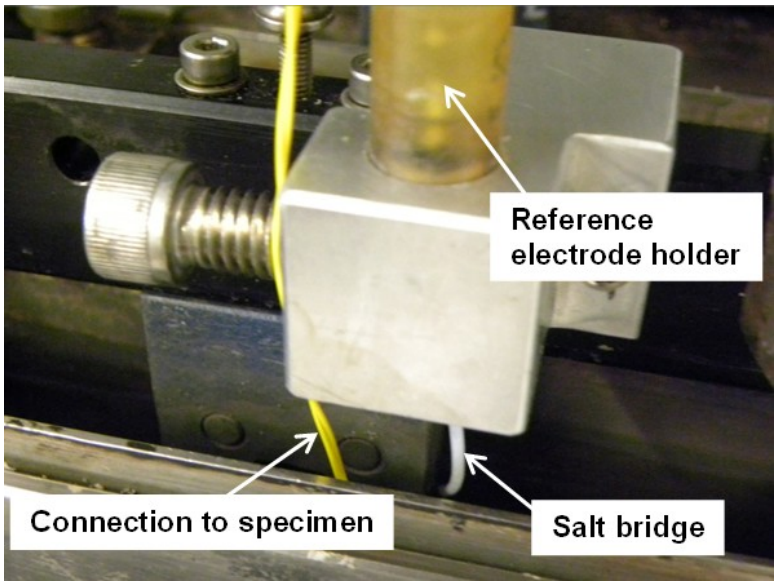

(b)

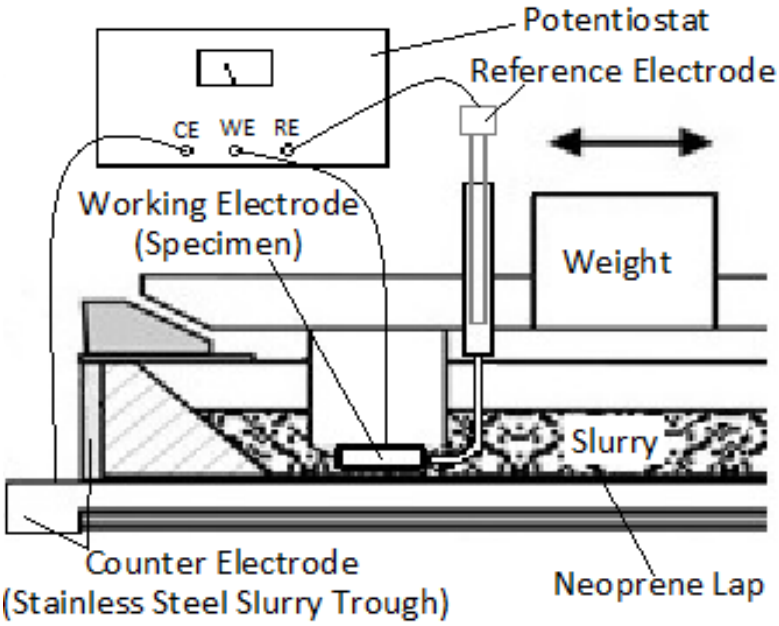

(c)

Fig. 2 Setup of the in-situ electrochemical cell (a), the salt bridge from the reference electrode holder to the testing slurry (b), and schematic diagram (c)

The holder for the reference electrode is filled with 1M potassium chloride solution, which is bridged to the testing slurry by a plastic tube filled with 1M potassium chloride gellified with agar as shown more clearly in Fig. 2b. The end of the plastic tube salt bridge is fixed on to the specimen holder and is placed as close as possible to the testing surface of the wear specimen. The stainless steel body of the slurry trough is used as the counter electrode. The in-situ electrochemical cell is schematically shown in Fig. 2c.

Using this set up, slurry abrasion testing can be performed both with and without cathodic protection (CP) to investigate the abrasion-corrosion synergy as per the ASTM G119 Standard Guide [28].

For specimens to be tested under cathodic protection (for abrasion-only loss measurement), a connection wire is first spot-welded on the back surface of the specimen opposite to the test surface (Fig. 3a). Then, the surfaces other than the testing surface (i.e., the bottom of the specimen) are coated with an isolation paint to eliminate corrosion from the non-testing surfaces (Fig. 3b). To prevent the damage of the isolation coating during the abrasion testing (on the side surfaces), the specimen is further protected with a shrinkable plastic tube (Fig. 3c).

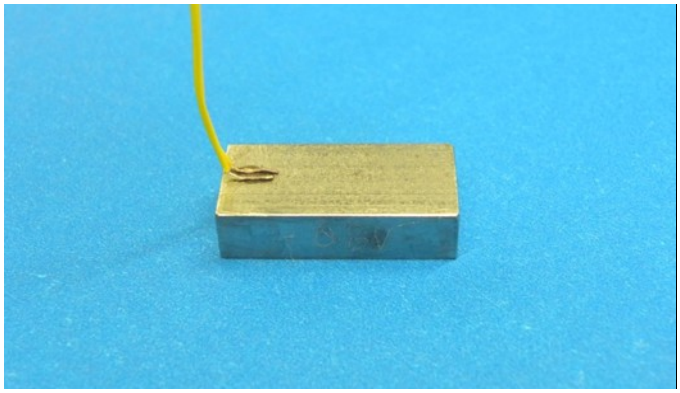

(a)

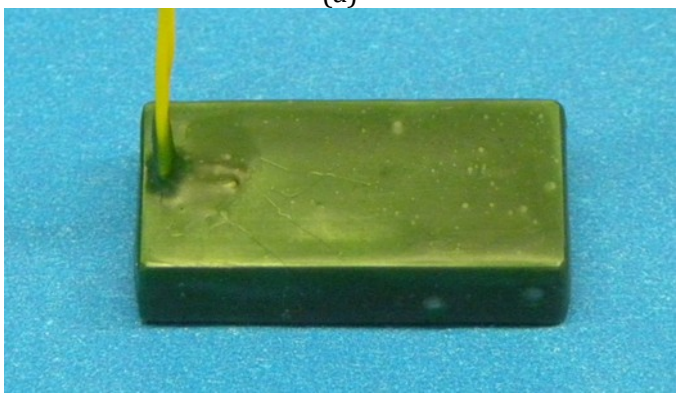

(b)

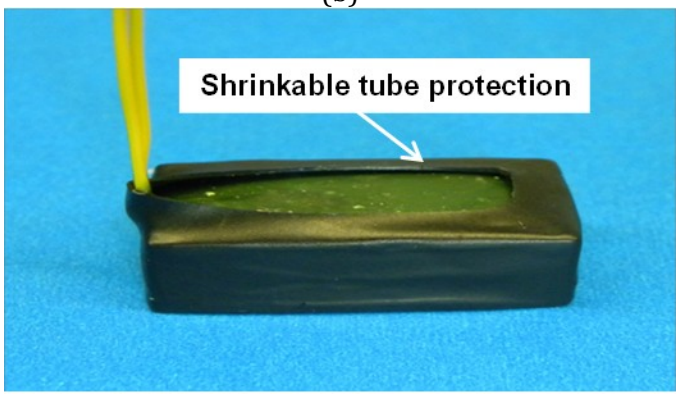

(c)

Fig. 3 Wear specimen preparation for testing under cathodic protection

2.2 Slurry abrasion response (SAR) number calculation

Based on ASTM G75 standard [27], the wear rate of the material is expressed using the slurry abrasion response (*SAR*) number, which is defined by

$$SAR = 18.18\left(\frac{dM}{dt}\Big|_{t=2hr}\right)\left(\frac{7.58}{\rho_{sample}}\right) \quad (1)$$

where ρ_{sample} is the density of the material under investigation, and M (in mg) the cumulative mass loss at different sliding time, t (in hr).

The definition for *SAR* number in Eq. (1) is for sliding at the standard speed of 48 rpm. The cumulative mass loss, M, is obtained by measuring sample mass changes at three equally spaced 2 hr testing intervals, i.e., at a total/accumulated sliding time, t, of 2 hr, 4hr, and 6 hr respectively. A curve fitting is conducted for a relationship (Eq. 2) between the cumulative mass loss, M, and sliding time, t, from which the mass loss rate, $dM/dt|_{t=2hr}$, at two hours' sliding is obtained and used for the calculation of *SAR* number in Eq. 1:

$$M = A\,t^{B} \quad (2)$$

where A and B are fitting constants.

3. Experimental Validation of the Methodology

3.1 Experimental details

For validation of the methodology, a preliminary experimental study was performed on QT 100 steel using the testing system. The material is a type of quenched and tempered steel, similar to ASTM A514, and has a hardness of 28.7 HRC (equivalent to 283 HV). The testing surface of a specimen was wet polished with silicon-carbide sandpapers, with a final finish using 400-Grit one.

The testing slurry is made of AFS 50/70 silica sand and a liquid. The liquid for making the slurry is either deionized (DI) water or 3.5% NaCl (salt) solution. Two slurry concentrations, 50 wt% of sand (150g sand + 150 mL liquid) and 10 wt% of sand (20g sand + 180 ml liquid) respectively, are used. Slurry pH value was monitored before the onset of each test. The pH is around 7.1 to 7.2 for all the slurry compositions.

The sliding speed is either 48 rpm (0.325 m/s, the standard speed as per ASTM Standard) or 16 rpm (0.108 m/s). The load on the wear specimen is 22.2 N. For specimens tested at the speed of 48 rpm, the test lasted for a total of six hours, and the mass loss was measured after every two hours of testing. When using the sliding speed of 16 rpm, the total test duration lasted for 18 hours, and mass loss of the specimen was measured after every 6 hours of testing. That way, the total sliding distance, as well as that between two measurements, is kept the same independent of the sliding speed. The total sliding cycles are 5760 cycles in both cases.

To make the results comparable, equivalent *SAR* numbers are obtained for the sliding speed of 16 rpm, and each time interval of 6 hr at 16 rpm is considered equivalent to 2 hr at 48 rpm.

For catholically protected wear testing, the specimen was immersed into the slurry and kept at the ready position for ten minutes while the open circuit potential was measured. A cathodic potential of 0.5 V more negative to the open circuit potential was then applied before starting the slurry abrasion testing.

3.2 Results and discussion

The cumulative mass losses versus the cycles of sliding are shown in Fig. 4, based on which the respective SAR number has been calculated and listed in Table 1.

It can be seen that the abrasive wear rate (as expressed by the *SAR* numbers) are dependent on the slurry corrosivity (water or salt solution), concentration of solids in slurry, and sliding speed. Overall, it is evident that the abrasive wear rate increases with slurry concentration and corrosivity but inversely with sliding speed.

As shown in Fig 4, after the cathodic protection is applied, cumulative mass loss is significantly reduced, and the large difference observed without cathodic protection is mostly eliminated. This is a strong indication that wear mass loss is mostly due to pure mechanical abrasion under cathodic protection. It should be noted that, under cathodic protection, the cumulative mass losses are slightly higher in slurry of DI water than those in slurry of salt solution of similar solid particle concentration; this is because the cathodic protection is less effective in slurry of DI water, due to lower electric conductivity. In fact, lower cathodic polarization current was observed in slurry with DI water.

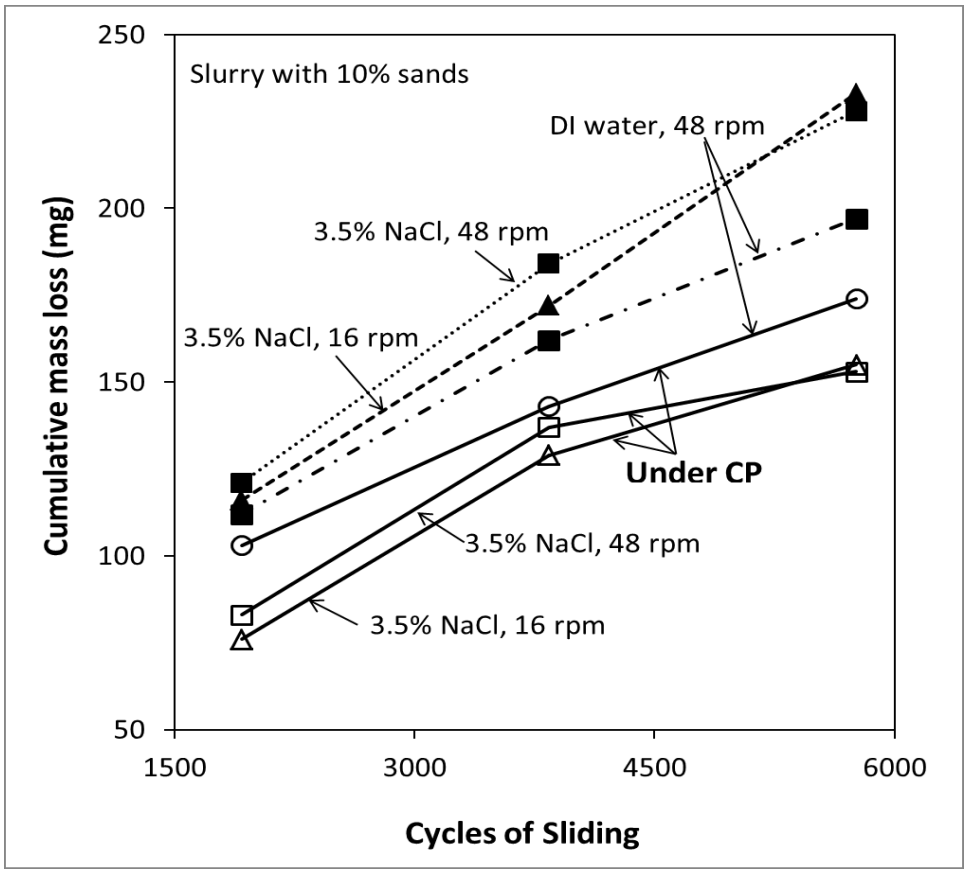

(a)

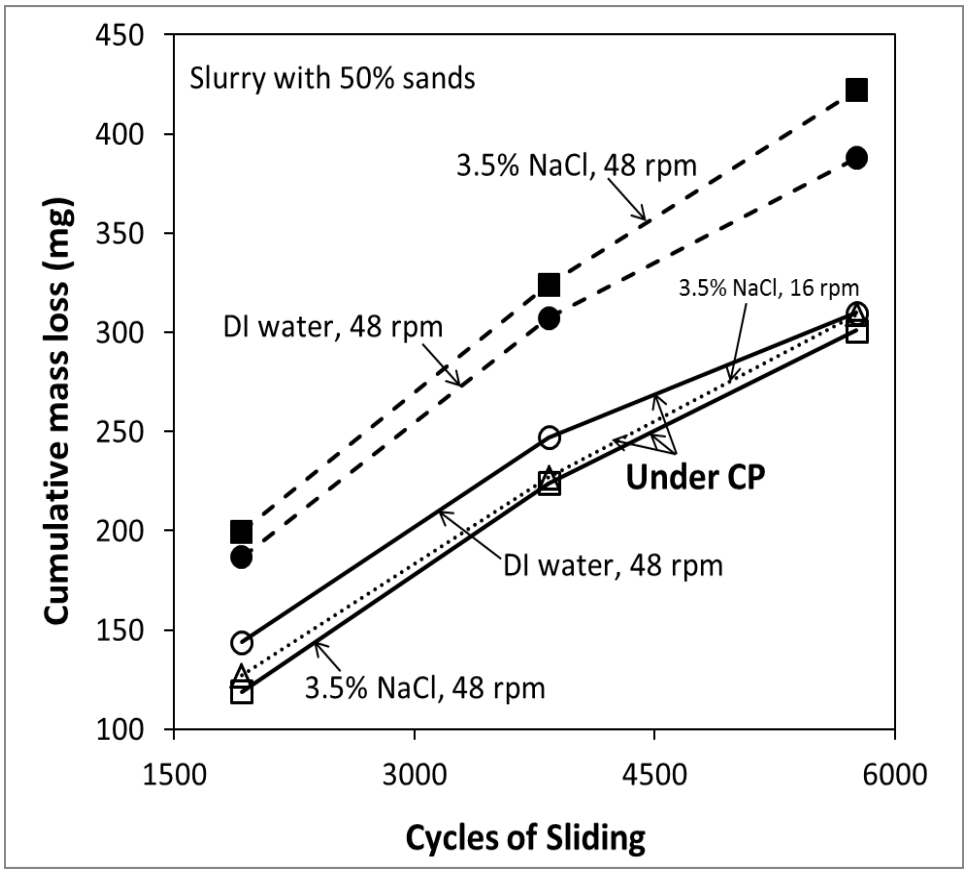

(b)

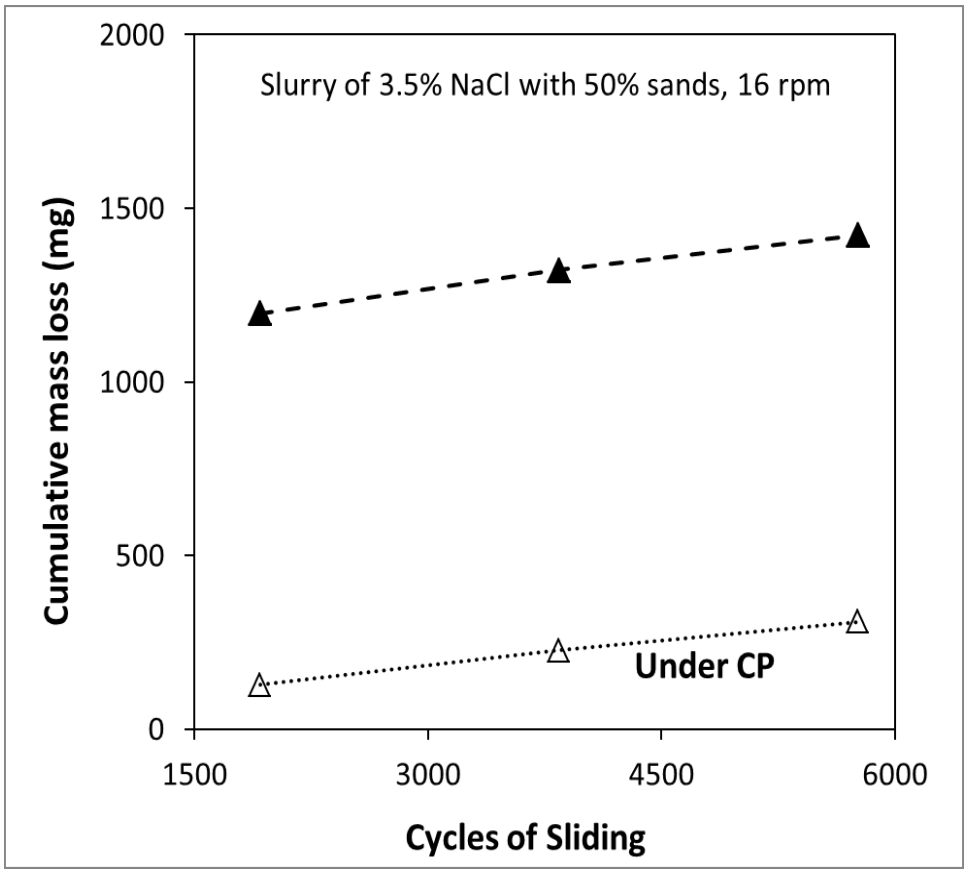

(c)

Fig. 4 Reduction of cumulative mass loss (versus the cycles of sliding) under cathodic protection.

Table 1: *SAR* numbers under different testing conditions and the ratio of corrosion enhancement

Condition or Note	Slurry with 50% sands			Slurry with 10% of sands		
	DI Water, 48 rpm	3.5% NaCl, 48 rpm	3.5% NaCl, 16 rpm	DI Water, 48 rpm	3.5% NaCl, 48 rpm	3.5% NaCl, 16 rpm
Without CP	1026	1238	1409	526	625	683
With CP	943	944	961	458	436	463
Contribution ratio of pure mechanical wear (%)	92	76	68	87	70	68
SAR enhancement ratio by corrosion (%)	8	24	32	13	30	32

Considering a general tribo-corrosion system, the total wear rate, T, can be considered as a sum of pure mechanical wear loss rate, W_0, corrosion rate in the absence of wear, C_0, and the synergistic component, S, as follows:

$$T = W_0 + C_0 + S \quad (3)$$

The pure corrosion loss rate, C_0, can be easily measured in a separate corrosion cell using electrochemical method. With the above established abrasion-corrosion test system, the total wear rate, T, can be measured during sliding abrasion tests without cathodic protection, while the pure mechanical wear loss rate, W_0, can be obtained under cathodic protection. On that basis, the total synergy, S, can be derived. The wear rate can be well reflected by the corresponding *SAR* numbers.

As the main purpose of the current study is to introduce and demonstrate the new abrasion-corrosion testing system and methodology, the pure corrosion term was not separately measured. Instead, the sum of pure corrosion rate and the synergistic component, i.e., $C_0 + S$, were combined together and reported in Table 1 as a contribution of corrosion to the total material loss rate, the "SAR enhancement ratio by corrosion".

The effectiveness of cathodic protection eliminating corrosion contribution to the wear loss rate (i.e., $C_0 + S$) can also been seen from the results listed in Table 1. Under cathodic protection, the SAR number (i.e., the wear rate) seems to be only a function of sand concentration in the slurry and is independent of the slurry corrosivity and sliding speed.

When testing was conducted in the low corrosivity slurry with deionized water, the SAR enhancement ratio by corrosion is only about 10% with slight differences depending on the solid concentration in the slurry (Table 1).

If the slurry is made of the salt solution, the slurry corrosivity is significantly higher. Compared to the slurry with DI water, the slurry with NaCl provides Na^+ and Cl^- irons, which increase the conductivity of the slurry, promoting both anodic and cathodic half-cell reactions and thus increasing the electrochemical corrosion rate. In addition, Cl^- ion also attacks the protective oxide layer (if any) formed on the surface, promoting corrosion reaction. Consequently, the enhancement of wear rate by corrosion is increased.

Sliding speed also showed evident effect on the total material loss as well as on the relative contribution of corrosion. Slower sliding increases the SAR enhancement ratio by corrosion. However, in the present situation, the effect of slurry corrosivity is more significant.

With regard to effect of solid concentration in the slurry, both the total material loss rate and pure mechanical wear rate are much lower for a slurry with lower solid concentration (i.e., for the slurry with 10% of sands as compared to the one with 50% of sands), but the difference in SAR enhancement ratio by corrosion is less significant.

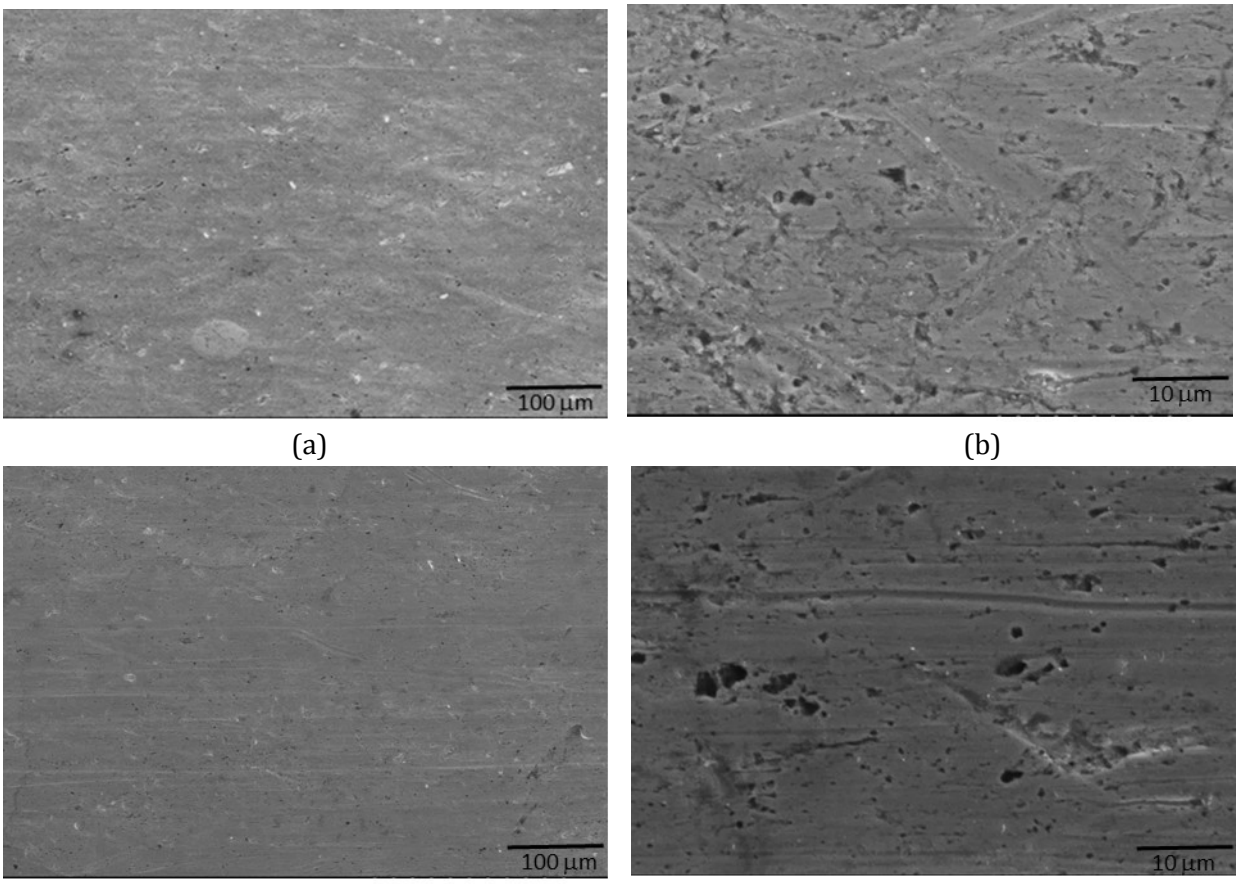

Fig. 5 Surface appearances of a specimen after testing in 3.5% NaCl slurry with 10wt% sands under sliding speed of 48 rpm (a and b: without CP; c and d: under cathodic protection).

Wear surfaces after testing under the various conditions are relatively flat, as shown in Figs. 5 and 6. Some local plastic deformation due to micro-plowing or wedging could be observed at higher magnification. In all the cases, small pits can be observed. The pits on the specimens tested under cathodic protection appear to be more defined and deeply developed (as shown in respective micrographs in Figs. 5 and 6). Pitting initiation is possible under abrasion due to associated micro surface deformation, as it is well known that pits can preferentially nucleate/form along scratches or plastically deformed regions for iron [29, 30]. Under cathodic protection, it is believed that, overall, general corrosion is depressed, where the likelihood of sustained growth of pits (once initiated) is higher; in contrast, if general corrosion prevails, small shallow pits could be eliminated by uniform corrosion, and the likelihood of sustained growth of pits will be lower.

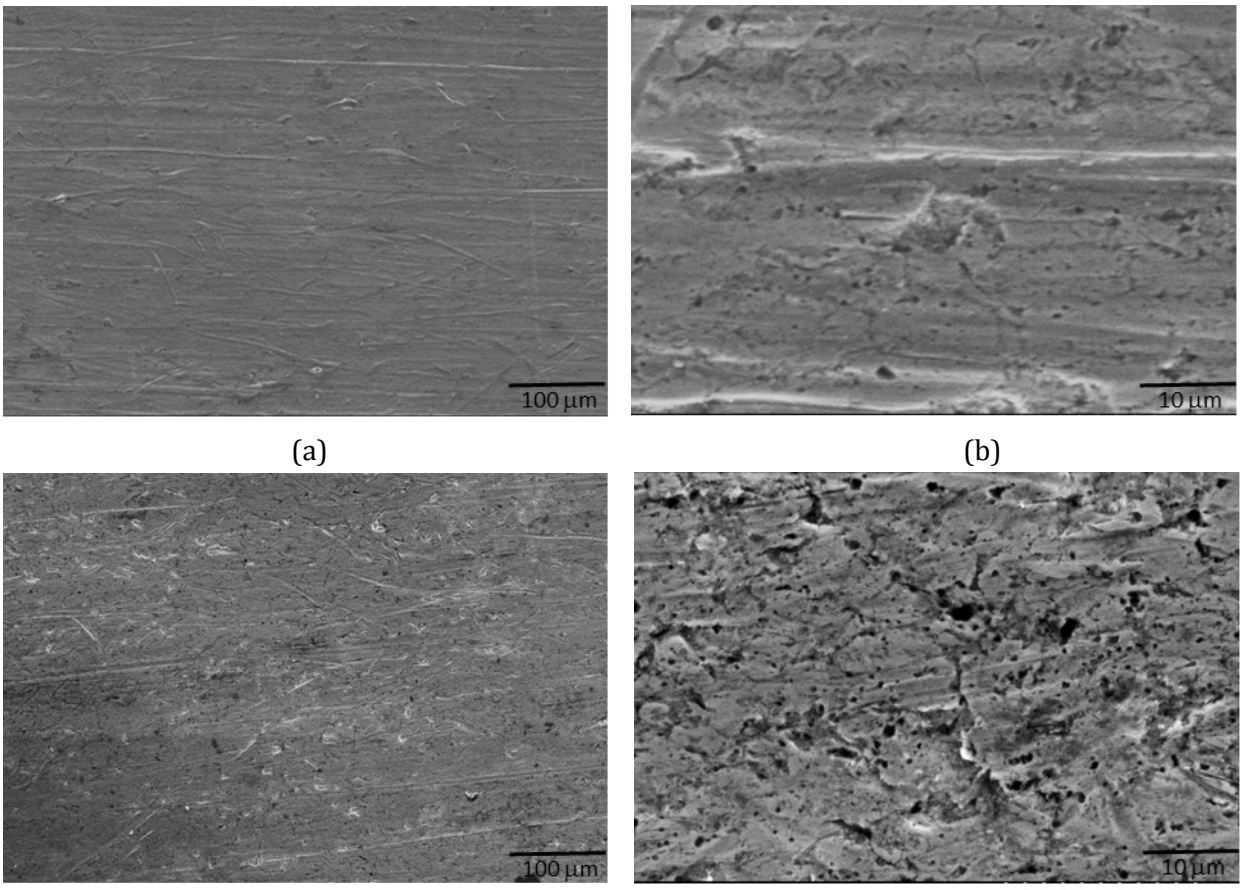

Fig. 6 Surface appearances of a specimen after testing in 3.5% NaCl slurry with 50wt% sands with sliding speed of 16 rpm (a and b:without cathodic protection; c and d: under cathodic protection).

A detailed discussion of slurry abrasion corrosion mechanism is out of the scope. In general, during slurry abrasion with Miller tester, low stress abrasion occurs. QT 100 steel has much lower hardness as compared with silica particles. Consequently, against abrasion by silica sands, localized surface deformation (in a form of micro-plowing and/or micro–wedging) and related work hardening can occur, leading to microfatigue and/or microcracking over time. Furthermore, corrosion can promote abrading, such as by forming localized damages to facilitate microcracking or by forming the thin oxide layer that is more readily abradable. On the other hand, localized surface deformation and work hardening cause higher state of disorder and result in larger microscopic surface area, which can enhance corrosion rate; sliding can increase mass transfer, and abrasion can remove protective oxide film, both promoting corrosion.

4. Conclusions

A methodology has been developed to study the abrasion-corrosion synergism in slurry abrasion by incorporating an in-situ three-electrode electrochemical cell to a Miller tester. The following conclusions can be drawn from this investigation:

- Preliminary experimental investigation using methodology developed on QT 100 steel indicate that the slurry abrasion corrosion and the synergy can be effective investigated.
- Cathodic protection (employing 0.5 V more negative to the open circuit potential) in the established system setup is effective in eliminating the corrosion effect during slurry abrasion testing, allowing a reliable measurement of pure abrasion component for analyzing abrasion-corrosion synergism.
- The abrasive wear rate in slurry abrasion is dependent on solid concentration in the slurry, slurry corrosivity, and sliding speed (i.e., the time of exposure to the slurry).
- Corrosion-induced enhancement on slurry abrasion loss rate increases with slurry corrosivity but inversely with sliding speed
- Slurry corrosivity appears to play a more significant role in corrosion-induced enhancement on wear rate as compared to sliding speed.

Conflict of Interests Declaration:

On behalf of all authors, the corresponding authors state that there is no conflict of interest.

5. References

[1] Tian BR, Cheng YF (2008) Electrochemical corrosion behavior of X-65 steel in the simulated oil sand slurry. I: Effects of hydrodynamic condition. Corrosion Science 50:773–779.

[2] Tang X, Xu LY, Cheng YF (2008) Electrochemical corrosion behavior of X-65 steel in the simulated oil–sand slurry. II: Synergism of erosion and corrosion. Corrosion Science 50:1469–1474.

[3] Yu B, Li DY, Grondin A (2013) Effects of the dissolved oxygen and slurry velocity on erosion–corrosion of carbon steel in aqueous slurries with carbon dioxide and silica sand. Wear 302:1609–1614.

[4] Parent LL, Li DY (2013) Wear of hydrotransport lines in Athabasca oil sands. Wear 301:477–482.

[5] Jones M, Llewellyn RJ (2009) Erosion–corrosion assessment of materials for use in the resources industry. Wear 267:2003–2009.

[6] Jones M, Waag U (2011) The influence of carbide dissolution on the erosion–corrosion properties of cast tungsten carbide/Ni-based PTAW overlays. Wear 271:1314– 1324.

[7] He DD, Jiang XX, Li SZ, Guan HR (2005) Erosion-Corrosion of Stainless Steels in Aqueous Slurries—A Quantitative Estimation of Synergistic Effects. Corrosion 61:30-36.

[8] Neville A, Hodgkiess T, Dallas JT (1995) A study of the erosion-corrosion behaviour of engineering steels for marine pumping applications. Wear 186–187:497–507.

[9] Toma D, Brandl W, Marginean G (2001) Wear and corrosion behaviour of thermally sprayed cermet coatings. Surface and Coatings Technology 138:149–158.

[10] Neville A, Reza F, Chiovelli S, Revega T (2004) Assessing MMCs for corrosion and erosion-corrosion applications in the oil sands industry. CORROSION/04, NACE, Paper 04125.

[11] Neville A, Hodgkiess T, Xu H (1999) An electrochemical and microstructural assessment of erosion–corrosion of cast-iron. Wear 233–235:523–534.

[12] Clark HM (1993) The influence of flow field in slurry erosion. Wear 152:223–240.

[13] Souza VAD, Neville A (2007) Aspects of microstructure on the synergy and overall material loss of thermal spray coatings in erosion–corrosion environments. Wear 263:339–348.

[14] Yang Y, Cheng YF (2012) Parametric effects on the erosion–corrosion rate and mechanism of carbon steel pipes in oil sands slurry. Wear 276– 277:141– 148.

[15] Rajahram SS, Harvey TJ, Wood RJK (2009) Erosion–corrosion resistance of engineering materials in various test conditions. Wear 267:244–254.

[16] Jana BD, Stack MM (2005) Modelling impact angle effects on erosion–corrosion of pure metals: construction of materials performance maps. Wear 259:243–255.

[17] Meng H, Hu X, Neville A (2007) A systematic erosion–corrosion study of two stainless steels in marine conditions via experimental design. Wear 263:355–362.

[18] Mischler S, Debaud S, Landolt D (1998) Wear-Accelerated Corrosion of Passive Metals in Tribocorrosion Systems. J. Electrochem. Soc. 145:750-758.

[19] Jemmely P, Mischler S, Landolt D (2000) Electrochemical modeling of passivation phenomena in tribocorrosion. Wear 237:63–76.

[20] Jiang J, Stack MM (2006) Modelling sliding wear: From dry to wet environments. Wear 261:954–965.

[21] García I, Drees D, Celis JP (2001) Corrosion-wear of passivating materials in sliding contacts based on a concept of active wear track area. Wear 249:452–460.

[22] Landolt D, Mischler S, Stemp M, Barril S (2004) Third body effects and material fluxes in tribocorrosion systems involving a sliding contact. Wear 256:517–524.

[23] Jiang J, Stack MM, Neville A (2002) Modelling the tribo-corrosion interaction in aqueous sliding conditions. Tribology International 35:669–679.

[24] Guo HX, Lu BT, Luo JL (2005) Interaction of mechanical and electrochemical factors in erosion–corrosion of carbon steel. Electrochimica Acta 51:315–323.

[25] Barik RC, Wharton JA, Wood RJK, Stokes KR (2009) Electro-mechanical interactions during erosion–corrosion. Wear 267:1900–1908.

[26] Jiang J, Tufa KY (2013) The Effect of Corrosion on Slurry Abrasion of Wear Resistant Steels. In: Blau PJ, Celis J-P, Drees D (eds) Tribo-Corrosion: Research, Testing, and Applications. ASTM Selected Technical Papers STP1563, pp. 66-87.

[27] ASTM G75 - 07 Standard Test Method for Determination of Slurry Abrasivity (Miller Number) and Slurry Abrasion Response of Materials (SAR Number), 2007. (DOI: 10.1520/G0075-07)

[28] ASTM G119 – 09, 2009, "Standard Guide for Determining Synergism Between Wear and Corrosion", ASTM International, West Conshohocken, PA, 2009, DOI: 10.1520/G0119-09.

[29] Vetter KJ, Strehblow HH (1974) Pitting corrosion in an early stage and its theoretical implications. In: U.R. Evans-Conference on Localized Corrosion. Williamsburg 1971, NCE Houston 1974, pp. 240-251.

[30] Weil KG, Menzel D (1959) Die Einwirkung von Halogenionen auf pas- sives Eisen (The action of halide ions on passive iron). Z. Elektrochem 63:669-673.